

Temperature distribution in a panel-radiant heating system

Jurabek Kamolov ^{1,*} and Kamoliddin Samiev ²

¹ *Department of Heliophysics, Renewable Energy Sources and Electronics, Bukhara State University, 200117, M. Ikbol st., Bukhara, Uzbekistan.*

² *Department of Physics, Bukhara State University, 200117, M. Ikbol st., Bukhara, Uzbekistan.*

International Journal of Science and Research Archive, 2025 14(02), 1617-1625

Publication history: Received on 16 January 2025; revised on 22 February 2025; accepted on 25 February 2025

Article DOI: <https://doi.org/10.30574/ijrsra.2025.14.2.0560>

Abstract

In this study, a computer model was developed in Comsol Multiphysics to determine and evaluate the temperature distribution in a panel-radiant heating system with a heated floor. A panel-radiant heating system consisting of a concrete layer with dimensions of $4 \times 3.3 \times 0.1 \text{ m}^3$ was selected, and copper pipes with an inner diameter of 2 cm and total lengths of 64.84 m and 64.24 m were installed within this volume. Water was used as the heat carrier. The calculations revealed that in the second configuration, the temperature distribution on the surface of the panel-radiant heated floor system is relatively uniform and does not exceed the required value.

Keywords: Panel-Radiant Heating System; Thermal Properties; Analytical Solution; Temperature Distribution; Thermal Resistance

1. Introduction

Due to the rapid growth of the global population, residential buildings, and industrial enterprises, the demand for fossil fuel energy sources such as natural gas, coal, and oil has sharply increased. Consequently, the reserves of these underground resources are depleting at an alarming rate. The combustion of fossil fuels, classified as underground resources, significantly increases the concentration of greenhouse or toxic gases such as NO_2 , SO_2 , and CO_2 in the atmosphere. These gases may lead to a deviation of the average global temperature from desired levels and result in a sharp rise in toxic gas concentrations in the air [1].

The rapid growth of the global economy and the continuous improvement of living standards have progressively exacerbated global energy crises and environmental pollution [2]. Residential buildings account for 30-40% of total global energy consumption [3]. In Uzbekistan, 40% of total energy consumption is attributed to energy losses from residential buildings and apartments [4], which indicates that the amount of heat energy consumed in residential buildings is 2-4 times higher than in certain developed countries [5].

To achieve the required indoor thermal comfort, various heating systems can be employed, such as forced air heating, seat-based heating, radiant floor heating with panels, and convector heating. However, relative humidity poses risks to the objects placed within the room [6]. Over the years, various solutions to these issues have been developed, and utilizing renewable energy sources has emerged as a promising direction. Renewable energy sources include solar, wind, geothermal, hydropower, and more. Among them, solar energy is preferred for its cost-effectiveness, availability in most regions worldwide, minimal environmental impact, ease of use, efficiency, and high technical potential. Studies suggest that by 2050, the share of solar energy used for heating buildings will significantly increase [7].

* Corresponding author: Jurabek Kamolov

Radiant floor heating systems efficiently provide thermal comfort, maintain consistent vertical room temperatures, and ensure a uniform temperature distribution. This is due to the optimal angular coefficient of radiant floors compared to other surfaces such as ceilings, windows, and walls. Consequently, radiant floor systems allow for nearly uniform temperatures across vertical layers and horizontal surfaces, outperforming other heating methods [8-9].

In recent years, solar heating systems based on renewable energy, integrated with radiant floor heating systems, have gained widespread adoption across various sectors for heating residential and commercial buildings. A major advantage of these systems is their ability to create comfortable indoor temperatures across horizontal and vertical layers while utilizing low-temperature heat carriers. When coupled with parabolic solar concentrators, radiant floor heating can reduce annual energy consumption by up to 26%, with a payback period ranging from 18 to 22.5 years, depending on heat loss prevention measures [10-12].

A.J. Verner-Juszczuk [13] analyzed the effect of aluminum layer thickness on lightweight radiant floor heating systems using ANSYS Steady-State Thermal Solver (Workbench 19.2). Aluminum thicknesses between 0.1 mm and 0.5 mm were evaluated for water temperature, pipe spacing, and constructions. Results indicated that water temperatures of 25-30°C with 0.3-0.5 mm aluminum layers are effective for tiled structures, while temperatures of 25-35°C with 0.3-0.4 mm aluminum layers are optimal for wooden structures.

R. M. S. F. Almeida et al. [14] experimentally and digitally simulated radiant heating systems, assessing various materials, floor coverings, and coating solutions. They found a 15% efficiency difference in surface temperatures due to coating materials.

Low-temperature radiant heating systems [15] were compared to conventional radiators and three radiant floor heating modes, with calculations verified by laboratory measurements. The energy consumption for radiant heating exceeded that of radiators, with a significant energy consumption difference of up to 23.2%-24.8% in nearly zero-energy buildings.

In recent years, the use of radiant floor heating and cooling systems for residential buildings, shopping complexes, and educational institutions has advanced significantly. For instance, in Europe, 50-60% of newly constructed buildings utilize radiant floor heating and cooling [16].

To support energy simulations, a radiant heating and cooling model has been developed. A. Laouadi [17] evaluated radiant floor systems as a promising technology to reduce energy costs and enhance thermal comfort in energy-intensive buildings. These systems aim to lower thermostat temperatures during winter and raise them during summer, offering substantial energy savings compared to conventional systems. Some studies show that radiant heating can achieve energy savings exceeding 30% [18-20].

In addition to energy savings, radiant floor heating systems provide superior thermal comfort, making them efficient and advantageous [21-22]. About 64-67% of heat transfer in these systems occurs via radiation, while 33-36% is due to natural convection [23]. This ensures consistent temperature distribution within the space and reduces cold air movement [24-25]. Furthermore, radiant floor heating systems save space, enhance interior design aesthetics, and eliminate noise issues, making them highly desirable [26].

Yongqiang Luo, Ling Zhang et al. [27] examined the dynamic thermal performance of radiant floor systems, optimizing design by considering aluminum panel conductivity, insulation thickness, electrical resistance, and Seebeck coefficient. They concluded that aluminum panel thicknesses of 1-2 mm, insulation thicknesses of 40-50 mm, and consistent placement of thermoelectric modules (TEMs) on radiant floor surfaces yielded optimal results.

Several effective practices have been developed for radiant floor systems, including geometric optimization, efficient pipe layouts, condensation drainage systems, and personalized heating zones within large areas. These aspects, along with the system's advantages and limitations, have been analyzed [28].

This study investigates the thermal distribution and different configurations of radiant floor systems.

2. Material and methods

Mathematical model. The temperature distribution in the radiant floor heating system was calculated using a computer model developed in the **Comsol Multiphysics** software environment [29]. The computer model is based on the following equations. The energy equation for a solid concrete structure is expressed as follows:

$$\rho C_p \frac{\partial T}{\partial t} + \rho C_p u \cdot \nabla T + \nabla \cdot q = Q + Q_{\text{ted}} \quad \dots \dots (1)$$

here ρ -density; C_p - heat capacity; T - temperature; t -time; u -velocity; Q -heat quantity.

$$q = -k \nabla T \quad \dots \dots \dots (2)$$

here q - heat flow; k - thermal conductivity coefficient.

The energy equation for the pipe is expressed as follows:

$$\rho A C_p \frac{\partial T}{\partial t} + \rho A C_p u_{\text{et}} \cdot \nabla T = \nabla_t (A k \nabla_t T) + \frac{1}{2} f_D \frac{\rho A}{d_h} |u| u^2 + Q + Q_{\text{wall}} \quad \dots \dots (3)$$

here f_D - hydraulic resistance; d_h - hydraulic diameter; A - cross-sectional area.

The initial and boundary conditions for these equations are as follows:

- The velocity of the heat carrier entering the pipe is 0.1 m/s.
- At the initial time, the system temperature is 20°C (Figure 1).
- The thermophysical parameters of the radiant floor heating system elements were adopted based on Table 1.
- The indoor air temperature is 20 °C.
- The heat carrier temperature at the system inlet is set to 90°C and 55°C.
- The relative error in the calculations was assumed to be 0.01.

To solve equations (1)-(3), the study object was discretized into finite elements in the Comsol Multiphysics environment. The total number of elements was 16,142. The computation, performed on a computer with a 2.10 GHz processor and 32 GB RAM, took an average of 1,726 seconds.

The following sequence is used for modeling the research object in the **Comsol Multiphysics** environment:

- Using the **“Model Wizard”** command, the modeling dimension is selected first. The dimension can be one-dimensional, two-dimensional, or three-dimensional, depending on the physical processes occurring in the research object.
- The **“Select Physics”** command is used to choose the model for the physical processes occurring in the research object.
- The **“Select Study”** command is used to define the time dependency of the process. The process can be stationary or non-stationary.
- In the **“Global Definitions”** section of the **“Model Builder”**, the **“Parameters”** section is used to input constants or parameters related to the research object.
- The **“Geometry”** section is used to draw the geometric shape of the research object.
- In the **“Materials”** section, materials are assigned to the components of the research object.
- Boundary conditions are applied for the selected physical models.
- Using the **“Mesh”** command, a mesh is selected for the research object.
- In the **“Study”** section, the computation type is chosen, and the calculations are performed.
- In the **“Results”** section, the obtained results are presented in various graphical formats, and data is generated for further analysis.

Description of the research object. For the calculations, a radiant floor heating system (heated floor) consisting of a concrete layer with dimensions of $4 \times 3.3 \times 0.1 \text{ m}^3$ was selected. The inner diameter of the pipe used is 2 cm, with a total pipe length of 64.84 m for version 2a and 64.24 m for version 2b. The thermal-physical properties of the concrete and pipe are presented in Table 1. The temperature-dependent values of the thermal-physical properties were interpolated and utilized in the calculations using the Comsol Multiphysics software.

Table 1 Thermal-physical properties of materials [30].

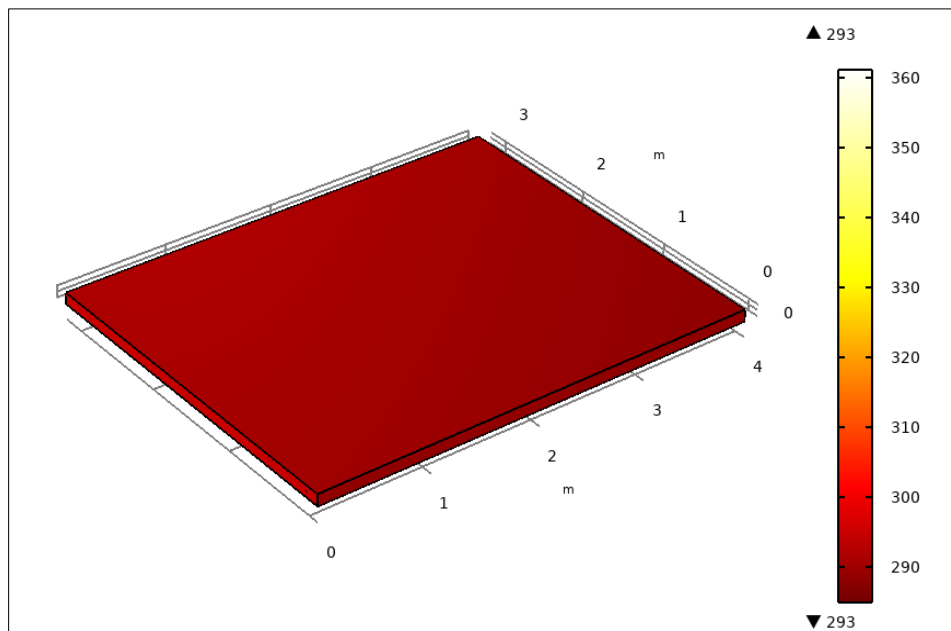
Material	Thermal conductivity coefficient, W/(m· K)	Specific heat capacity, J/(kg· K)	Density, kg/m ³
Concrete	1.8	880	2300
Copper	1.75	840	2400

The pipe is placed at the center of the concrete along its height and is installed in two different configurations (Figure 3a and 3b). Water was used as the heat transfer fluid inside the pipe. Changes in the thermophysical properties of water with temperature variations were taken into account.

3. Results and discussion

Figure 1 shows the underfloor heating section of the panel radiant heating system under investigation. The temperatures on the surface of the underfloor heating system at the end of the calculations are presented in Figure 2 (a, b, c, d). A comparison of the figures reveals that, under the given boundary conditions, the temperature distribution across the entire surface is more uniform in Figures 2b and 2d compared to Figures 2a and 2c.

The temperature distribution along the length of the pipe at the end of the calculations is shown in Figure 3a and 3b. When the inlet water temperature is 90 °C and the flow velocity is 0.1 m/s, the outlet water temperature is 45.9 °C in the configuration shown in Figure 2a and 43.9 °C in the configuration shown in Figure 2b. On the surface of the underfloor heating, the maximum temperature is 87.9°C and the minimum temperature is 14.9 °C in Figure 2a, while in Figure 2b, the maximum temperature is 87.9 °C and the minimum temperature is 15.9 °C. The total amount of heat transferred per second is 5816 J in the configuration shown in Figure 2a and 6080 J in the configuration shown in Figure 2b. It is evident that when the temperature of the water entering the pipe is 90 °C, the surface temperature of the underfloor heating exceeds the required level [31].

**Figure 1** The panel radiant heating system in its initial state

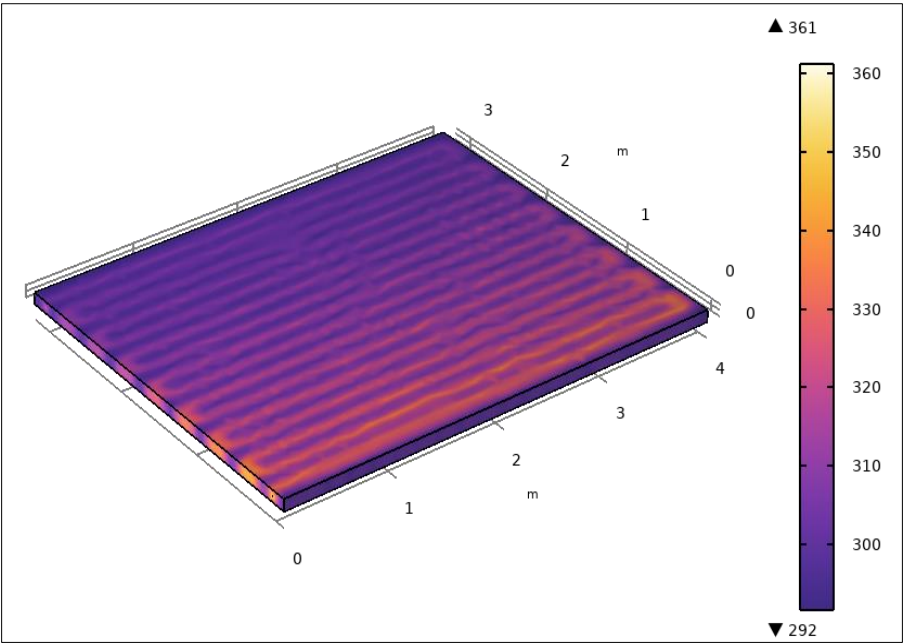


Figure 2a The arrangement of pipes in the first configuration for panel radiant heating, as well as the visualization for the case where the inlet temperature is 90 °C

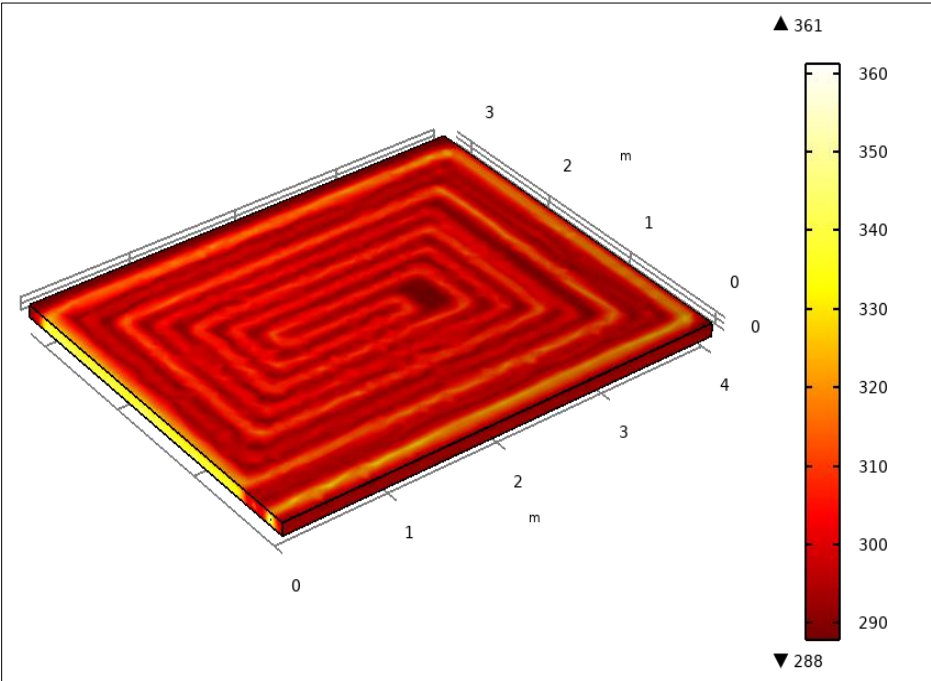


Figure 2b the arrangement of pipes in the second configuration for panel radiant heating, as well as the visualization for the case where the inlet temperature is 90 °C.

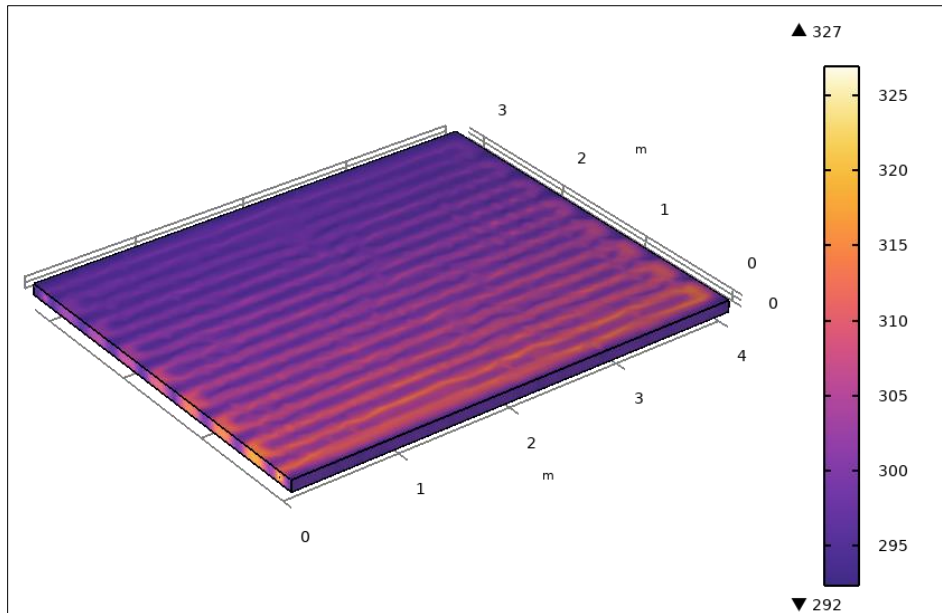


Figure 2c. The arrangement of pipes in the first configuration for panel radiant heating, as well as the visualization for the case where the inlet temperature is 55 °C

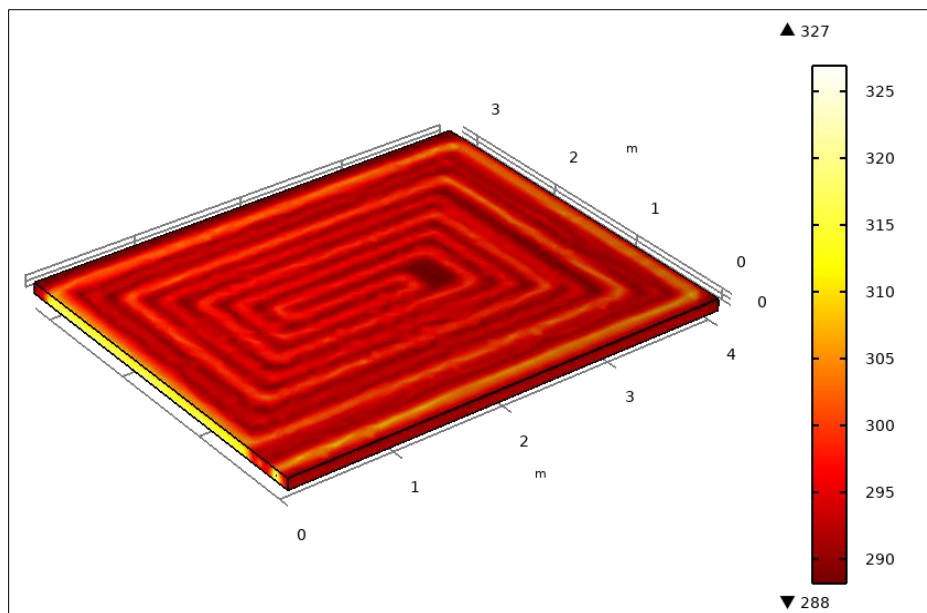


Figure 2d. The arrangement of pipes in the second configuration for panel radiant heating, as well as the visualization for the case where the inlet temperature is 55 °C

The temperature distributions of the panel radiant heating system were examined above. In the panel radiant heating system, when the temperature of the heat transfer fluid (water) entering the underfloor heating pipe is 55 °C, as shown in Figure 2c, the minimum temperature is 18.9 °C and the maximum temperature is 53.9 °C. In Figure 2d, the minimum temperature is 15 °C and the maximum temperature is 54 °C. In this case, when the temperature of the heat transfer fluid (water) entering the pipe is 55 °C, the average surface temperature of the underfloor heating does not exceed the required value.

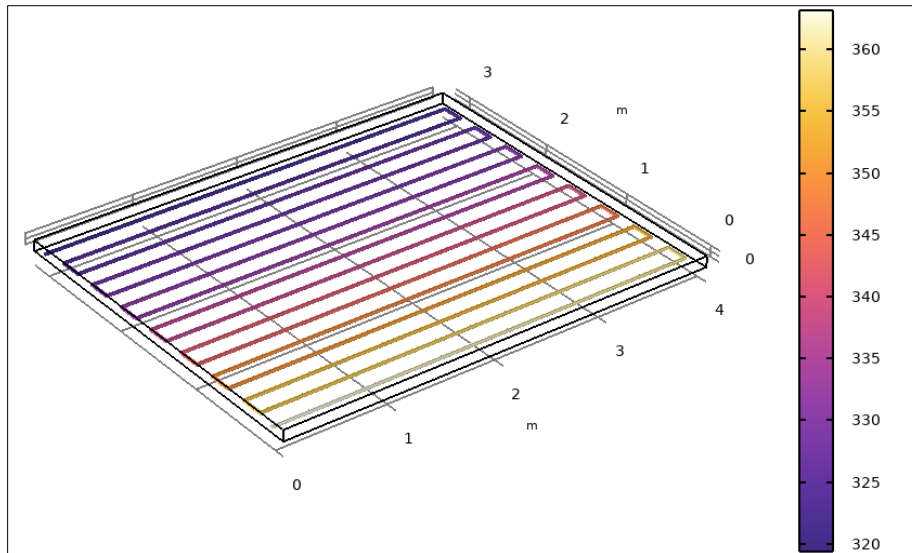


Figure 3a Temperature distribution in the pipes of the first configuration installed in the panel radiant heating system at the end of the calculation

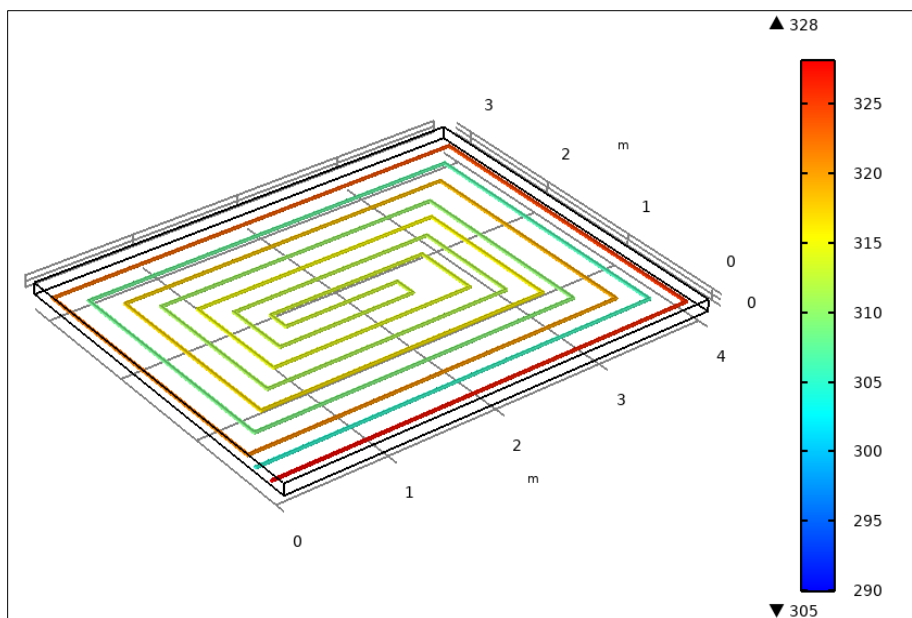


Figure 3b Temperature distribution in the pipes of the second configuration installed in the panel radiant heating system at the end of the calculation

4. Conclusion

In the research, the COMSOL Multiphysics computer software was used. A panel radiant heating system (underfloor heating) consisting of a concrete layer with dimensions of $4 \times 3.3 \times 0.1 \text{ m}^3$ was selected, and copper pipes with an inner diameter of 2 cm, a total length of 64.84 m, and 64.24 m were placed within this volume. Water was used as the heat transfer fluid in the calculations. Copper pipes were placed inside the underfloor heating layer under two conditions, and the temperature distributions on their surfaces, as well as the temperatures along the lengths of the copper pipes within the underfloor heating system, were investigated. When the temperature of the incoming water in the pipes was 90°C , the maximum temperature was 87.9°C and the minimum temperature was 14.9°C , as shown in Figure 2a, while in Figure 2b, the maximum temperature was 87.9°C and the minimum temperature was 15.9°C . This indicates that when the temperature of the heat transfer fluid (water) entering the underfloor heating pipe is 90°C , the surface

temperature of the underfloor heating exceeds the required level, leading to a disruption in comfort conditions. When the temperature of the heat transfer fluid (water) entering the pipe is 55 °C, as shown in Figure 2c, the minimum temperature is 18.9 °C and the maximum temperature is 53.9 °C. In the panel radiant heating system, a relatively uniform temperature distribution across the entire surface can be observed in the variant shown in Figure 2d. Here, the minimum temperature is 15 °C and the maximum temperature is 54 °C, and in this case, the average surface temperature of the panel radiant underfloor heating does not exceed the required value. The calculations show that in the second variant, the temperature distribution on the surface of the panel radiant underfloor heating system is relatively uniform and does not exceed the required value.

Compliance with ethical standards

Disclosure of conflict of interest

No conflict of interest to be disclosed.

References

- [1] Reza Karimi, Touraj Tavakoli Gheinani, Vahid Madadi Avargani, A detailed mathematical model for thermal performance analysis of a cylindrical cavity receiver in a solar parabolic dish collector system, *Renewable Energy* (2018), doi: 10.1016/j.renene.2018.03.015
- [2] Y. Lin et al. A novel variable speed ASHP frosting suppression operation method based on the frosting suppression performance map [J] *Appl. Therm. Eng.* (2023), doi.org/10.1016/j.applthermaleng.2023.121254
- [3] G. Martinopoulos, K.T. Papakostas, A.M. Papadopoulos, A comparative review of heating systems in EU countries, based on efficiency and fuel cost, *Renew. Sustain. Energy Rev.* 90 (2018) 687–699, doi.org/10.1016/j.rser.2018.03.060
- [4] Samiev K.A., Halimov A.S., Fayziev Sh.Sh. Multiobjective Optimization of Integration of the Trombe Wall in Buildings Using a Full Factorial Experiment // *Applied Solar Energy. –USA. 2022. –Vol.58, №1. –pp.127-136 (№3, CiteScore, IF=2.5).*
- [5] Samiev K.A., Mirzaev M.S., Ibragimov U.X. Annual thermal performance of a passive solar heating system with a Trombe wall with phase change materials // *IOP Conference Series: Earth and Environmental Science.* 2022. Vol.1070, doi:10.1088/1755-1315/1070/1/012022 (№3, CiteScore, IF=0.6).
- [6] W. Uyttenhove, M. De Paepe, A. Janssens. CFD-modelling of temperature and humidity distribution in the St. Pieter's Church. IAE Annex 41, Subtask 1, Meeting May 12-14 (2004) Zürich.
- [7] E. Taibi, D. Gielen, M. Bazilian. The potential for renewable energy in industrial applications, *Renewable and Sustainable Energy Reviews* 16(1) (2012) 735-744, doi.org/10.1016/j.rser.2011.08.039
- [8] X. Liu, T. Zhang, X. Liu, L. Li, L. Lin, Y. Jiang, Energy saving potential for space heating in Chinese airport terminals: The impact of air infiltration, *Energy.* 215 (2021) 119175, doi.org/10.1016/j.energy.2020.119175
- [9] B.W. Olesen. Radiant floor heating in theory and practice. *ASHRAE Journal.* July (2002) 19–24.
- [10] Cho J., Park B., Lim T. Experimental and numerical study on the application of low-temperature radiant floor heating system with capillary tube: Thermal performance analysis. *Applied Thermal Engineering* 163 (2019) 114360, doi.org/10.1016/j.applthermaleng.2019.114360
- [11] Laouadi A. Development of a radiant heating and cooling model for buildingenergy simulation software / *Building and Environment* 39 (2004) 421–431.
- [12] Kamolov, J.J., Mirzayev, M.S., Fayziyev, Sh.Sh., Samiev, K.A. Use of paraboloid solar concentrators to reduce heat consumption of residential buildings in the climatic conditions of Uzbekistan / *BIO Web of Conferences.*, 2024, 84, 05019.
- [13] A. J. Werner-Juszczuk, "The influence of the thickness of an aluminium radiant sheet on the performance of the lightweight floor heating," *Journal of Building Engineering*, vol. 44, no. June, p. 102896, 2021, doi: 10.1016/j.jobbe.2021.102896
- [14] R. M. S. F. Almeida et al., "Experimental and Numerical Simulation of a Radiant Floor System: The Impact of Different Screed Mortars and Floor Finishings," *Materials*, vol. 15, no. 3, 2022, doi: 10.3390/ma15031015.

- [15] T. Kalmár, B. Bodó, and F. Kalmár, "Heat losses of low-temperature radiant heating systems," *Energy Reports*, vol. 10, pp. 1982–1995, 2023, doi: 10.1016/j.egy.2023.08.090.
- [16] Kilikis BI, Sager SS, Uludag M. A simplified model for radiant heating and cooling panels. *Simulation Practice and Theory* 1994;2:61–76.
- [17] A. Laouadi, "Development of a radiant heating and cooling model for building energy simulation software," *Building and Environment*, vol. 39, no. 4, pp. 421–431, 2004, doi: 10.1016/j.buildenv.2003.09.016
- [18] Stetiu C. Energy and peak power potential of radiant cooling systems in US commercial buildings. *Energy and Buildings* 1999;30:127–38.
- [19] Feustel HE, Stetiu C. Hydronic radiant cooling—preliminary assessment. *Energy and Building* 1995;22:193–205.
- [20] Yost PA, Barbour CE, Watson R. An evaluation of thermal comfort and energy consumption for a surface mounted ceiling radiant panel heating system. *ASHRAE Transactions* 1995;101(1):1221–35.
- [21] X.L. Hao et al. A combined system of chilled ceiling, displacement ventilation and desiccant dehumidification. *Build environ* (2007)
- [22] O. Acikgoz. A novel evaluation regarding the influence of surface emissivity on radiative and total heat transfer coefficients in radiant heating systems by means of theoretical and numerical methods. *Energy Build* (2015)
- [23] T. Imanari et al. Thermal comfort and energy consumption of the radiant ceiling panel system: comparison with the conventional all-air system. *Energy Build* (1999)
- [24] R.A. Memon et al. Thermal comfort assessment and application of radiant cooling: a case study. *Build Environ* (2008)
- [25] B. Ning et al. Cooling capacity improvement for a radiant ceiling panel with uniform surface temperature distribution. *Build Environ* (2016)
- [26] O. Acikgoz. A novel evaluation regarding the influence of surface emissivity on radiative and total heat transfer coefficients in radiant heating systems by means of theoretical and numerical methods. *Energy Build* (2015)
- [27] Yongqiang Luo, Ling Zhang et al. Dynamic heat transfer modeling and parametric study of thermoelectric radiant cooling and heating panel system. *Energy Conversion and Management*, 124, 9 2016 doi.org/10.1016/j.enconman.2016.07.055
- [28] Michal Krajčík, Zuzana Straková, Müslüm Arıcı, Tomasz Cholewa. Techniques to improve the performance of hydronic radiant heating and cooling panels by geometry modification, personalisation and increasing air convection. *Energy and Buildings* 6 January 2025, 115272 doi.org/10.1016/j.enbuild.2025.115272 <https://doc.comsol.com/5.5/doc/com.comsol.help.heat/HeatTransferModuleUsersGuide.pdf>.
- [29] KMK 2.01.04-2018 "Construction Thermal Engineering", Tashkent, 2018.
- [30] SanPiN No. 0331-16. Sanitary rules and regulations for the design, construction, and maintenance of residential buildings in the climatic conditions of Uzbekistan, 2016.